

Rothamsted Repository Download

A - Papers appearing in refereed journals

Sun, F., Suen, P. K., Zhang, Y., Liang, C., Carrie, C., Whelan, J., Ward, J. L., Hawkins, N. D., Jiang, L. and Lim, B. L. 2012. A dual-targeted purple acid phosphatase in *Arabidopsis thaliana* moderates carbon metabolism and its overexpression leads to faster plant growth and higher seed yield. *New Phytologist*. 194 (1), pp. 206-219.

The publisher's version can be accessed at:

- <https://dx.doi.org/10.1111/j.1469-8137.2011.04026.x>

The output can be accessed at: <https://repository.rothamsted.ac.uk/item/8q9xx>.

© Rothamsted Research. Licensed under the Creative Commons CC BY.

A dual-targeted purple acid phosphatase in *Arabidopsis thaliana* moderates carbon metabolism and its overexpression leads to faster plant growth and higher seed yield

Feng Sun¹, Pui Kit Suen¹, Youjun Zhang¹, Chao Liang¹, Chris Carrie², James Whelan², Jane L. Ward³, Nathaniel D. Hawkins³, Liwen Jiang⁴ and Boon Leong Lim¹

¹School of Biological Sciences, the University of Hong Kong, Pokfulam, Hong Kong, China; ²Australian Research Council Centre of Excellence in Plant Energy Biology, University of Western Australia, Crawley WA 6009, Australia; ³National Centre for Plant and Microbial Metabolomics, Rothamsted Research, West Common, Harpenden, Herts, AL5 2JQ, UK; ⁴School of Life Sciences, Centre for Cell and Developmental Biology, the Chinese University of Hong Kong, Hong Kong, China

Summary

Author for correspondence:

Boon Leong Lim
Tel: +852 22990826
Email: bllim@hku.hk

Received: 18 October 2011
Accepted: 28 November 2011

New Phytologist (2012) **194**: 206–219
doi: 10.1111/j.1469-8137.2011.04026.x

Key words: chloroplasts, flowering, mitochondria, purple acid phosphatase (PAP), sucrose phosphate synthase, sugars, TCA.

- Overexpression of AtPAP2, a purple acid phosphatase (PAP) with a unique C-terminal hydrophobic motif in *Arabidopsis*, resulted in earlier bolting and a higher seed yield. Metabolite analysis showed that the shoots of AtPAP2 overexpression lines contained higher levels of sugars and tricarboxylic acid (TCA) metabolites. Enzyme assays showed that sucrose phosphate synthase (SPS) activity was significantly upregulated in the overexpression lines. The higher SPS activity arose from a higher level of SPS protein, and was independent of SnRK1.
- AtPAP2 was found to be targeted to both plastids and mitochondria via its C-terminal hydrophobic motif. Ectopic expression of a truncated AtPAP2 without this C-terminal motif in *Arabidopsis* indicated that the subcellular localization of AtPAP2 is essential for its biological actions.
- Plant PAPs are generally considered to mediate phosphorus acquisition and redistribution. AtPAP2 is the first PAP shown to modulate carbon metabolism and the first shown to be dual-targeted to both plastids and mitochondria by a C-terminal targeting signal.
- One PAP-like sequence carrying a hydrophobic C-terminal motif could be identified in the genome of the smallest free-living photosynthetic eukaryote, *Ostreococcus tauri*. This might reflect a common ancestral function of AtPAP2-like sequences in the regulation of carbon metabolism.

Introduction

Modification of carbon (C) metabolism is a prime target for maximizing crop productivity (Sharma-Natu & Ghildiyal, 2005). Sugars not only represent an energy product from photosynthesis, but also play roles in complex cellular signaling pathways (Rolland *et al.*, 2002, 2006; Gibson, 2005), which are mediated by a variety of protein kinases (PKs), and protein phosphatases (PPs) (Baena-Gonzalez & Sheen, 2008; Smeekens *et al.*, 2010; Zheng *et al.*, 2010). In *Arabidopsis thaliana*, SNF1-related kinase (SnRK1) is a central resource regulator in response to energy deficiency (Baena-Gonzalez *et al.*, 2007). By phosphorylating and inactivating sucrose phosphate synthase (SPS), nitrate reductase (NR), and a few other metabolic enzymes (Lunn & MacRae, 2003; Polge *et al.*, 2008), energy and resources were reallocated from anabolic pathways (e.g. sucrose synthesis and nitrogen assimilation) to catabolic pathways (Smeekens *et al.*, 2010). In *Arabidopsis*, geminivirus Rep interacting kinases

(GRIK1 and GRIK2) activate SnRK1 by phosphorylating it at the T₁₇₅ residue (Shen & Hanley-Bowdoin, 2006; Shen *et al.*, 2009).

PPs regulate a variety of genes involved in sugar metabolism, such as those encoding the two major amylases of the tuberous root of sweet potato (Takeda *et al.*, 1994), the ADP-glucose pyrophosphorylase subunit in sweet potato and *Arabidopsis* (Takeda *et al.*, 1994; Siedlecka *et al.*, 2003), and the enzymes for fructan synthesis (Martinez-Noel *et al.*, 2009), the UDP-glucose pyrophosphorylase, and the sucrose synthase of *Arabidopsis* (Winter *et al.*, 1997; Ciereszko *et al.*, 2001; Martinez-Noel *et al.*, 2009). Okadaic acid, a PP inhibitor, prevents activation of SPS and impairs sucrose accumulation in leaves (Huber *et al.*, 1992). Okadaic acid also induces vacuolar acid invertase transcription, suggesting that PP activity plays a role in C partitioning (Martinez-Noel *et al.*, 2009).

Purple acid phosphatases (PAPs) represent a large group of nonspecific acid phosphatases (Schenk *et al.*, 2000). In the

Arabidopsis genome, 29 PAP genes have been identified based on sequence comparison (Zhu *et al.*, 2005). Plant PAPs are considered to mediate phosphorus acquisition and redistribution based on their ability to hydrolyze phosphorus compounds (Cashikar *et al.*, 1997; Lung *et al.*, 2008; Kuang *et al.*, 2009). Certain PAPs also exhibit peroxidase activity, such as GmPAP3 (Liao *et al.*, 2003; Li *et al.*, 2008) and AtPAP17 (del Pozo *et al.*, 1999). Recent studies also showed that a tobacco PAP (NtPAP12) can modulate polysaccharide synthesis; it can upregulate β -glucan synthesis and cellulose deposition in the cell wall by dephosphorylating α -xylosidase and β -glucosidase (Kaida *et al.*, 2009, 2010).

In this study, we show that AtPAP2 is dual-targeted to mitochondria and plastids via a novel and unique C-terminal transmembrane targeting signal. Overexpression of AtPAP2 significantly enhanced the growth rate and seed yield of Arabidopsis, through increased SPS activity.

Materials and Methods

Plant materials and growth conditions

Wild-type (WT) *Arabidopsis thaliana* (L.) Heynh. ecotype Columbia (Col-0) was used in this study. The T-DNA mutant of AT1G13900 (Salk_013567, ecotype Col-0) and AT2G03450 (Salk_129905, ecotype Col-0) were obtained from The Arabidopsis Information Resource (TAIR, <http://www.arabidopsis.org>). Chilled Arabidopsis seeds were surface-sterilized with 20% (v/v) bleach for 15 min, washed, and plated on Murashige and Skoog (MS) medium supplemented with 2% (w/v) sucrose for 10 d. Seedlings with the same size were transferred to soil under a 16-h light (22°C) : 8-h dark (18°C) regime (long day, LD) or an 8-h light (22°C) : 16-h dark (18°C) regime (short day, SD) under a light intensity of 120–150 $\mu\text{mol m}^{-2} \text{s}^{-1}$. The pots were placed in the growth chamber in a randomized design. Bolting time was measured when the primary inflorescence reached 1 cm above the rosette leaves. This observation of phenotype was repeated at least three times ($n = 10\text{--}15$).

Sequence alignment and phylogenetic analysis

Sequence data was retrieved from the TAIR website (<http://www.arabidopsis.org>) and the National Center for Biotechnology Information (NCBI) (<http://www.ncbi.nlm.nih.gov>). Homology searches in GenBank were done using the Basic Local Alignment Search Tool server (<http://www.ncbi.nlm.nih.gov/BLAST/>). Multiple alignments of protein sequences were performed by MEGA 4.1 (Beta 3) software (Kumar *et al.*, 2004) (<http://www.megasoftware.net>) using the Clustal X and N-J plot programs (Saitou & Nei, 1987). The amino acid sequences were aligned by CLC sequence viewer 6.3 software (<http://www.clcbio.com>). Protein expression patterns were analyzed via the spot history microarray analysis tool (<http://www.affymetrix.com>). Arabidopsis.info/narrays/experimentbrowse.pl). Signal peptide and transmembrane motif were predicted by the SignalP and TMHMM programs (<http://www.cbs.dtu.dk/services>).

Generation of specific anti-AtPAP2 antiserum

A fragment of *AtPAP2* cDNA corresponding to the N-terminus of AtPAP2 (amino acids (a.a.) 25–144) was amplified by primers P2AbF and P2AbR. This region was selected to avoid cross-reactivity toward other AtPAPs. The PCR product was digested with *SacI* and *KpnI* and fused with the N-terminal His-tag of vector pRSET-A (Invitrogen, Hong Kong, China) and the resulting plasmids were transformed into *Escherichia coli* strain BL21 (DE3). The overexpressed fusion protein in the inclusion bodies was solubilized in extraction buffer A (20 mM Tris-HCl, pH 7.5, 150 mM NaCl, 8 M urea) and purified by a HisTrap FF column (GE Healthcare, Hong Kong, China) using buffer A containing 100 mM imidazole. The eluted protein was dialyzed in 20 mM PBS, pH 7.2 to remove urea. The antigen was further gel-purified before being used for rabbit immunization. The specificity of this antiserum was confirmed by western blotting analysis on the proteins isolated from WT and the T-DNA insertion line (Fig. S3d).

Expression of AtPAP2 under phosphate starvation and sugar treatments

Arabidopsis plants were grown in phosphate (Pi) starvation MS medium (0 mM Pi) for 5 d and then transferred to complete MS medium for 0, 2, 4, 6 or 8 d. Alternatively, plants were grown on MS agar for 7 d before transfer to Pi starvation medium for 0, 2, 4, 7 or 10 d (del Pozo *et al.*, 1999). For sugar treatments, 5-d-old seedlings on MS agar plates were transferred to solid MS medium containing a sucrose, glucose, sorbitol, or mannitol gradient (% w/v) for 24 h. Total protein isolated from seedlings was analyzed by western blot analysis using AtPAP2 antiserum.

Generation of AtPAP2 overexpression lines in Arabidopsis

The full-length coding region of the *AtPAP2* cDNA (AT1G13900) was amplified by Pfx DNA polymerase (Invitrogen, Hong Kong) using primers P2YF and P2NR. The resulting product (1971 bp) was initially cloned into vector pGEM-T Easy (Promega, Hong Kong, China) and then subcloned into the binary vector pBA002 downstream of the cauliflower mosaic virus (CaMV) 35S promoter (pBA002-CaMV35S: *AtPAP2*). The vector was then introduced into *Agrobacterium tumefaciens* strain GV3101 and then transformed by the floral dip method (Clough & Bent, 1998) into WT plants. Homozygous CaMV35S: *AtPAP2* overexpression (OE) lines were selected on MS plates containing 5 mg l^{-1} glufosinate ammonium (Sigma-Aldrich, St. Louis, USA). Resistant lines were transferred to soil to grow to maturity, and their transgenic status was confirmed by genomic PCR and western blot analyses. Homozygous T3 seeds of the OE plants were used for further analysis. A construct of a truncated *AtPAP2* fragment without its C-terminus (P2NC) was generated by PCR using primers P2YF and P2NCR and cloned in the pBA002 vector. *AtPAP2* with a deleted signal peptide (P2NS) was amplified with primers P2NSF and P2NR and cloned into the pCXSN vector (Chen *et al.*, 2009). All primers used are listed in Table S3.

Characterization of homozygous *AtPAP2* T-DNA line

A T-DNA insertion line of *AtPAP2* gene (Salk_013567) in the Col ecotype was obtained from TAIR. The homozygous T-DNA line was verified by genomic PCR screening using the T-DNA left border primer LBa1 and *AtPAP2* gene-specific primer LP2 and reverse primer RP2 (SIGnAL database). The T-DNA insertion site was confirmed by DNA sequencing of the PCR product.

Subcellular localization of AtPAP2

The putative signal peptide (SP) and the transmembrane domain and C-terminal tail (TMD/CT) were PCR-amplified from full-length *AtPAP2* cDNA and cloned into a GFP vector in pBI221 to generate SP-GFP, GFP-TMD/CT and SP-GFP-TMD/CT using full-length *AtPAP2* cDNA as template and the primer sets listed in Table S3. Organelle markers were used to elucidate the subcellular localization of *AtPAP2*-GFP constructs. Transient expression in WT Arabidopsis PSB-D cell culture was performed as described previously (Miao & Jiang, 2007). Generally, PSB-D cells at day 5 after subculture were collected for protoplast preparation. Plasmids were electroporated into protoplasts and incubated at 26°C for 13 h before being observed under a confocal laser scanning microscope. Protoplasts were incubated for 5 min at room temperature with MitoTracker Orange (CMTMRos; Invitrogen, Hong Kong, China) before analysis. Confocal images were collected with a Fluoview FV1000 microscope (Olympus, Tokyo, Japan) with a $\times 60$ objective water lens. The settings for collecting confocal images within the linear range were described previously (Tse *et al.*, 2004). Images were processed using Adobe Photoshop software.

Organelle isolation and western blot analysis

Mitochondria and chloroplasts were isolated from 10-d-old Arabidopsis seedlings as previously described (Lister *et al.*, 2007; Kubis *et al.*, 2008). Proteins (25 μ g) were resolved by SDS-PAGE and transferred to Hybond-C nitrocellulose membranes, then immunodetected as previously described (Carrie *et al.*, 2008). The antibodies used, Tom40 (Carrie *et al.*, 2009a,b) and Risp (Carrie *et al.*, 2010), have been described previously. Antibodies to CoxII, Rubisco large subunit and Rubisco small subunit (SSU) were purchased from Agrisera (Vännäs, Sweden).

Measurement of soluble sugars and starch in Arabidopsis

Soluble sugars were extracted from Arabidopsis using the chloroform/methanol method (Antonio *et al.*, 2007). Liquid chromatography-MS/MS spectrophotometry was employed for sugar measurement. Filtered samples (10 μ l) were injected into an HP 1100 HPLC system (Agilent Technologies, Palo Alto, CA, USA) connected to a zwitterionic ZIC-HILIC column (3.5 μ m, 150 mm \times 2.1 mm i.d.; SeQuant, Umea, Sweden) (Antonio *et al.*, 2008). Separation was performed using a solvent system of 0.1% (v/v) formic acid in water (A) and 0.1% (v/v) formic acid in methanol (B) with a linear gradient of 20–60% B over 25 min. Flow rate was maintained at 0.2 ml min⁻¹ and the elution was

monitored by a diode-array detector (200–600 nm). Multiple reaction monitoring (MRM) experiments were conducted at the electrospray ionization interface of an API 2000 QTRAP system (Applied Biosystems, Hong Kong, China) operating in negative mode. Starch measurement was carried out according to the method of Focks & Benning (1998) using a starch assay kit (Sigma-Aldrich, St. Louis, USA).

Enzyme assays

Sucrose synthase, soluble invertase and insoluble cell wall invertase activities were measured as described (Xu *et al.*, 1996; Dejardin *et al.*, 1997). SPS activity was assayed by the anthrone test (Lunn & Furbank, 1997; Baxter *et al.*, 2003). Acid phosphatase activity was assayed by a colorimetric method (Lung *et al.*, 2008) and the total NR activity assay was carried out as described (Yu *et al.*, 1998).

Pull-down assays using recombinant AtSnRK1.1, AtSnRK1.2, AtGRIK1, AtGRIK2 and 14-3-3 protein

Vectors for expressing GST-GRIK1, GST-GRIK2, His-AtSnRK1.1 (a.a. 1–341) and His-AtSnRK1.2 (a.a. 1–342) were gifts from Dr Shen Wei (Shen *et al.*, 2009). The expression vector GST-BMH1 (containing a yeast 14-3-3 homolog) was a gift from Prof. Carol MacKintosh (University of Dundee, UK). The fusion protein His-AtSnRK1.1/His-AtSnRK1.2 was purified by Ni-NTA beads and the fusion protein GST-GRIK1/GST-GRIK2 by a GST-Trap column (Amersham Biosciences) (Moorhead *et al.*, 1999). For His-AtSnRK1.1/His-AtSnRK1.2 pull-down assays, 20 μ g of protein in 200 μ l His binding buffer was coupled to 200 μ l of Ni-NTA beads and incubated with 1 mg total soluble Arabidopsis protein for 2 h at 4°C. The bound proteins were washed and eluted in binding buffer containing 100 mM imidazole. For the GST-GRIK1/GST-GRIK2 and GST-14-3-3 pull-down assays, 1 mg total plant protein extract was mixed with 5 μ g purified GST-fusion protein on 50 μ l GST beads with gentle agitation for 2 h at 4°C. The beads were washed with washing buffer (50 mM HEPES-KOH, pH 7.5, 500 mM NaCl, 1 mM dithiothreitol) five times. Bound proteins were eluted in 50 mM Tris-HCl, pH 8.0, 10 mM reduced glutathione, 500 mM NaCl and subjected to immunoblot analysis.

Analysis of proteins in AtPAP2 transgenic Arabidopsis plants

Total soluble proteins were extracted according to the trichloroacetic acid method (Zhu *et al.*, 2006). The samples were run in the pH 4–7 range and stained with SYPRO Ruby for total protein staining and Pro-Q Diamond for phosphoprotein staining. Images were analyzed using ImageMaster 2-D Platinum software (GE Healthcare, Hong Kong, China). The target spots were run on a MALDI-TOF/TOF mass spectrometer and identified by peptide mass fingerprinting with data searches carried out using MASCOT search tools (<http://www.matrixscience.com>) in the NCBI non-redundant public protein database. All of the peptide masses were assumed to be monoisotopic and corresponding to

[M⁺H⁺]. Carboxymethyl was considered to be a fixed modification, while Oxidation (M), Phospho (ST) and Phospho (Y) were considered variable modifications. The peptide mass tolerance was set at ± 0.2 Da and the maximum number of missed cleavages was set at one. The identified proteins had more than five matched peptides, and the percentage of sequence coverage was $> 20\%$. All of the positive protein identification scores were significant (MASCOT score > 60 , $P < 0.05$).

Metabolomic analysis by ¹H-NMR and GC-MS

Shoots of 20-d-old Arabidopsis were freeze-dried immediately after harvest. Three biological replicates were used in this study. For ¹H-NMR analysis, dried plant tissues (15 mg) were extracted at 50°C with D₂O : CD₃OD (80 : 20, 1 ml) containing 0.05% (w/v) d₄-TSP (Ward *et al.*, 2003; Beale *et al.*, 2010). NMR data was collected using 128 scans on a Bruker 600 MHz Avance NMR spectrometer (Bruker BioSpin, Coventry, UK) with a water suppression pulse sequence. Data was scaled to an internal standard (d₄-TSP) and binned to regions of equal width (0.01 ppm). For GC-MS analysis, lyophilized plant material (1.00 mg) was mixed with methoxyamine hydrochloride in anhydrous pyridine (50 μ l, 16 mg ml⁻¹, containing 40 μ g ml⁻¹ ribitol) and the samples were heated at 30°C for 90 min with agitation at 550 rpm. MSTFA + 1% TMCS (70 μ l) was then added and the sample was heated for 30 min at 37°C with agitation at 550 rpm. The derivatized samples were equilibrated at room temperature for 2 h before analysis. GC-MS analysis was carried out on a Pegasus III time of flight mass spectrometer (Leco Corp., St. Joseph, MI, USA) coupled to an Agilent 6890N gas chromatograph (Agilent Technologies) system fitted with a Microseal septum (Merlin Instrument Co., Newark, DE, USA), a FocusLiner port liner (SGE Analytical Science, Milton Keynes, UK) packed with deactivated quartz wool and a DB-5ms capillary column (15 m \times 0.18 mm I.D. \times 0.18 μ m d.f. with 5 m integrated guard column). Data were exported from ChromaTOF software as netCDF files and converted to MassLynx format using the DataBridge module of MassLynx v4.0 software (Waters, Elstree, UK) for semi-quantification in the QuanLynx module of MassLynx. A unique mass was assigned to each analyte observed in the dataset and its contribution (response factor) to the total ion current of its corresponding mass spectrum determined. For each analyte, peak areas for the unique mass were determined by integration of its corresponding extracted ion chromatogram, and the extracted ion chromatogram areas and response factors were used to calculate a reconstituted TIC peak area. Principal component analysis was carried out using Simca-P v.11 software (Umetrics, Umea, Sweden) with unit variance scaling. Significance was determined using ANOVA.

Results

Identification of a conserved class of PAP, with a C-terminal hydrophobic motif, in photosynthetic eukaryotes

AtPAP2 (AT1G13900) was classified as a group IIa PAP, among the 29 AtPAPs (Li *et al.*, 2002). The open reading frame of

AtPAP2 encodes a polypeptide of 656 amino acids with a predicted molecular weight of 73.72 kDa and a pI of 6.11. Database searches revealed that the protein contains a metallophosphoesterase domain within amino acids 256–487. In the genomic DNA, *AtPAP2* contains two exons. The program TMHMM predicts that AtPAP2 possesses a transmembrane motif at its C-terminus, suggesting that AtPAP2 is a membrane protein.

Phylogenetic analysis showed that PAPs with this C-terminal motif could only be found in plants, not in animals (Supporting Information Fig. S1). There are many more PAP-like sequences in the genomes of higher plants than in the genomes of primitive photosynthetic eukaryotes. For instance, there are 29 putative PAP genes in the genome of Arabidopsis (Li *et al.*, 2002) and two in *Ostreococcus tauri* (Fig. S1). Unlike Arabidopsis, where two PAPs contain a C-terminal hydrophobic region (AtPAP2 and AtPAP9), only a single PAP-like sequence from other plant genomes was found to carry this additional hydrophobic motif at the C-terminus (Figs S1, S2, Table S1). Interestingly, in the genome of the smallest free-living photosynthetic eukaryote, *O. tauri* (Derelle *et al.*, 2006), only two PAP-like sequences could be found among its 8166 ORFs, of which one (OtPAP2) carries a C-terminal hydrophobic motif (Table S1). In addition to this hydrophobic motif, all the sequences homologous to AtPAP2 carry an acidic amino acid doublet (e.g. EE, DD, ED) in the last 2–8 residues of the polypeptides (Table S1). These findings indicate that PAPs with a C-terminal hydrophobic motif are only found in photosynthetic eukaryotes, and have been conserved during the evolution of green plants.

Expression of AtPAP2 is not affected by phosphorus and sugar treatments

To examine the expression pattern of the AtPAP2 protein in various plant organs and at various developmental stages, a polyclonal antiserum was raised against recombinant AtPAP2 protein. A 74 kDa protein was detected in WT Arabidopsis but was absent in the T-DNA insertion line (Fig. S3). This indicates that the antiserum recognizes AtPAP2 specifically. AtPAP2 is highly expressed in siliques, stems, flowers, roots and senescing leaves, but its expression is relatively lower in leaves and mature seeds (Fig. S4). These results corroborate the results from RT-PCR experiments (Zhu *et al.*, 2005). Since AtPAP2 was predicted to be a constitutively expressed protein by spot history analysis (data not shown), the level of AtPAP2 protein expression under various stimuli was examined. As shown in Fig. S5, inorganic phosphate starvation, sucrose, glucose, sorbitol and mannitol treatments did not affect the level of AtPAP2, confirming that its expression is constitutive.

AtPAP2 overexpression accelerates plant growth and produces higher seed yield

A homozygous T-DNA line of *AtPAP2* that carries a T-DNA insertion site in the second exon (1864 bp/1971 bp) was identified (Fig. S3a). The insertion resulted in the loss of AtPAP2 expression, as indicated by the absence of detectable transcript

and protein (Fig. S3). Under normal germination conditions on MS agar, the length of hypocotyls of the *AtPAP2* T-DNA insertion line was shorter (*c.* 20–30%) than WT. To confirm whether the disruption of *AtPAP2* was responsible for the phenotype, the T-DNA insertion line was complemented by introducing the full-length coding sequence of *AtPAP2* into *Arabidopsis* under the control of the CaMV 35S promoter. Four homozygous lines were verified by western blot analysis and their hypocotyls were similar to WT seedlings (data not shown). Therefore, *AtPAP2* expression indeed rescued the short hypocotyl phenotype of the T-DNA line.

Overexpression studies were used to dissect the roles of *AtPAP2* *in vivo*. T3 homozygous *AtPAP2* OE transgenic lines under the control of CaMV 35S promoter were generated. Multiple independent lines with increased levels of *AtPAP2* protein, as confirmed by western blot analysis, were obtained. Two homozygous lines, OE7 and OE21, were randomly selected for subsequent studies. Compared to WT, both *AtPAP2* OE lines displayed earlier bolting (Fig. 1) and produced more lateral branches and inflorescences. Typically, *AtPAP2* OE plants started bolting earlier than both WT and the T-DNA line, *c.* 6 d earlier under LD growth conditions and *c.* 14 d earlier under SD conditions (Table 1a). At day 27 (LD) and day 41 (SD), when WT first bolted, *AtPAP2* OE lines had produced significantly more cauline leaves and inflorescences than WT (Fig. S6). Conversely, the number of rosette leaves of *AtPAP2* OE lines was fewer than WT (Fig. 1b, Table 1a), although the leaf area and total biomass of OE lines were similar to WT at 20 d old, at day 40, the total leaf area of *AtPAP2* OE lines was only 65% that of WT, but the total biomass was 2-fold higher than WT (Fig. 1c). *AtPAP2* OE plants not only matured earlier but also produced higher seed yields. In two independent experiments, the total seed yield of *AtPAP2* OE7 and OE21 plants increased remarkably by 40–57% over WT, which was due to higher numbers of auxiliary branches and a higher silique density (Table 1b). No significant differences in plant growth or seed yield relative to WT were observed in the *AtPAP2* T-DNA line, possibly due to redundancy of gene function.

AtPAP2 is dual-targeted to chloroplasts and mitochondria

The protein sequence of *AtPAP2* carries a hydrophobic C-terminal motif (TMD/CT) predicted to carry a trans-membrane motif and it has already been identified as a chloroplast protein by proteomics (Kleffmann *et al.*, 2004). By contrast, the SignalP server predicts that *AtPAP2* has a 24 amino acid SP at its N-terminus to direct the protein to the secretory pathway. To investigate the targeting of *AtPAP2*, 30 amino acid residues from the N-terminus and 69 amino acid residues from the C-terminus were fused to green fluorescent protein (GFP) under the control of the CaMV 35S promoter (Fig. 2a). Red fluorescence protein (RFP) was fused to either the mitochondrial presequence of the ATP synthase $F_1\text{-}\gamma$ subunit from *Nicotiana plumbaginifolia* ($F_1\text{-RFP}$) (Duby *et al.*, 2001) as a mitochondrial targeting marker or to the targeting sequence (a.a. 1–79) of the small subunit of tobacco Rubisco (plastid-mCherry) (Dabney-Smith *et al.*, 1999) as a

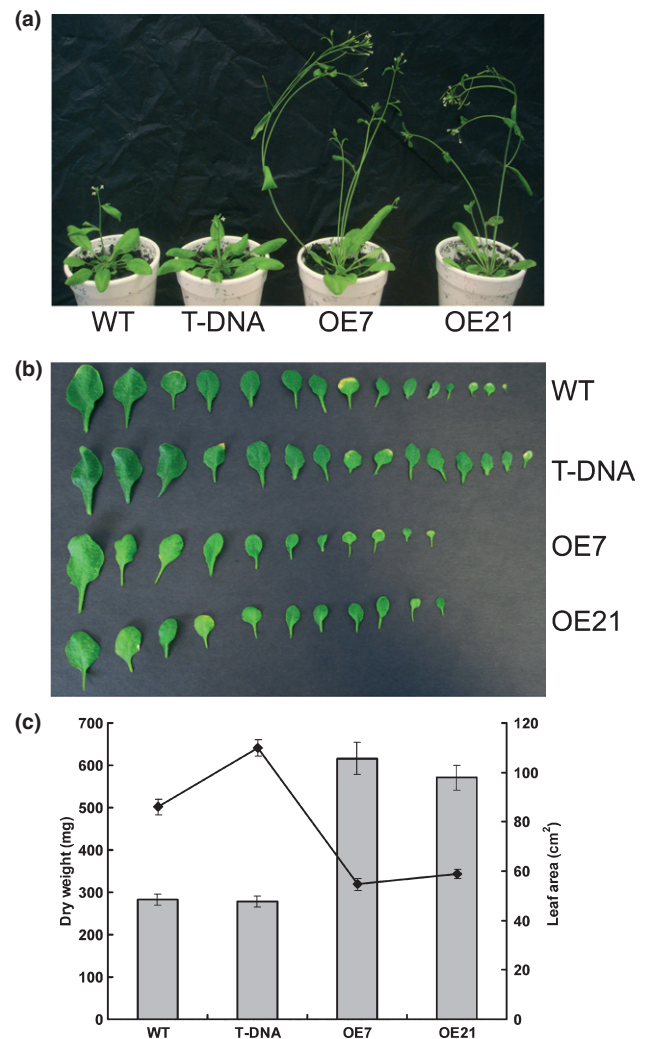


Fig. 1 Growth phenotypes of *AtPAP2* overexpression (OE) and T-DNA inactivation *Arabidopsis* lines. (a) Four-wk-old plants grown under long day (LD) conditions. (b) Leaves at day 27 under LD conditions. (c) Dry weight (bars) and total leaf area (line plot) of 40-d-old plants. *AtPAP2* OE lines exhibited higher biomass but much lower leaf area at age 40 d. Leaves were cut (including leaves on inflorescences, if any) and scanned. The leaf area was calculated using Metamorph Molecular Devices, Sunnyvale, CA, USA. The dry weights of individual plant samples (including leaves) were measured after water evaporation by heat. The experiments were repeated at least three times.

chloroplast targeting marker. Transient expression of the GFP fusion constructs was performed in WT *Arabidopsis* PSB-D cell culture (Fig. 2a).

Confocal microscopy analysis showed that both GFP (Fig. 2b,c, green) and GFP fused to the N-terminal SP (SP-GFP) (Fig. 2d,e, green) localized to the cytosol, and did not co-localize with the mitochondrial $F_1\text{-RFP}$ (Fig. 2b,d, red) or plastid-mCherry (Fig. 2c,e, red) markers. However, GFP constructs containing the TMD/CT region of *AtPAP2*, including SP-GFP-TMD/CT (Fig. 2f,g) and GFP-TMD/CT (Fig. 2h,i), were targeted to both plastids and to mitochondria, which were also labeled by the MitoTracker Orange (Molecular Probes) (Fig. S7). In addition, the patterns of expression of all GFP

Table 1 Growth phenotypes of transgenic *Arabidopsis*

(a) Bolting time				
Lines	Long day (LD, 16 h : 8 h)		Short day (SD, 8 h : 16 h)	
	AEI	NRL	AEI	NRL
WT	26.9 ± 1.2 ^a	13.0 ± 0.8 ^a	41.0 ± 4.7 ^a	18.0 ± 3.0 ^a
T-DNA	25.7 ± 0.7 ^a	11.6 ± 1.1 ^a	40.7 ± 4.9 ^a	15.0 ± 3.0 ^a
OE7	20.0 ± 1.1 ^b	6.4 ± 0.5 ^b	25.6 ± 1.3 ^b	5.3 ± 0.5 ^b
OE21	20.8 ± 0.6 ^b	6.5 ± 0.7 ^b	26.0 ± 1.1 ^b	5.4 ± 0.5 ^b

AEI, average date of emergence of inflorescence.
NRL, no. of rosette leaves at the first appearance of inflorescence.

(b) Seed yield at maturity			
Lines	No. of siliques per plant	Seed yield (g per plant)	Seed weight (mg per 100 seeds)
WT	396 ± 89 ^a	0.225 ± 0.058 ^a	1.96 ± 0.14 ^a
T-DNA	386 ± 70 ^a	0.240 ± 0.049 ^a	2.02 ± 0.16 ^a
OE7	621 ± 76 ^b	0.351 ± 0.050 ^b	1.91 ± 0.10 ^a
OE21	625 ± 94 ^b	0.355 ± 0.066 ^b	1.98 ± 0.03 ^a

All seeds and siliques from a single plant were harvested after the plant was completely dried. The plants were grown under LD regime.

(c) Carbohydrate contents in 20-d-old <i>Arabidopsis</i> shoots			
Lines	Sucrose (µg g ⁻¹ FW)	Hexose (µg g ⁻¹ FW)	Starch (mg g ⁻¹ FW)
WT	110.1 ± 33.3 ^a	16.7 ± 7.1 ^a	3.3 ± 0.4 ^a
T-DNA	116.1 ± 15.6 ^a	24.9 ± 7.3 ^a	4.4 ± 1.1 ^a
OE7	207.1 ± 22.5 ^b	43.9 ± 9.2 ^b	3.8 ± 1.0 ^a
OE21	147.7 ± 17.3 ^c	31.7 ± 4.8 ^{ac}	3.5 ± 0.8 ^a

Sugars were extracted 8 h after illumination during the LD regime from 20-d-old *Arabidopsis*.

Seeds of wild-type (WT), T-DNA line and two AtPAP2 overexpression (OE) lines (OE7 and OE21) were germinated in the MS agar for 10 d, seedlings with the same size were transferred to a growth chamber. Statistical differences ($P < 0.05$) in the same column for each line were based on one-way ANOVA analysis followed by Tukey's Honestly Significant Differences (HSD) test using statistical program SPSS 11.5. Within each column, the values marked by different letters (a, b, c) are significantly different ($P < 0.05$). There were 8–15 replicates for each line. The data were reproducible in at least two independent experiments.

constructs were distinct from that of the Golgi marker (RFP-ManI) (Cai *et al.*, 2011), ER marker (RFP-HDEL) (De Caroli *et al.*, 2011) (Fig. S8) and peroxisome marker (peroxisome-Cherry) (Nelson *et al.*, 2007) (Fig. S9). These results confirmed the importance of the TMD/CT in dual targeting of the reporter GFP protein to mitochondria and plastids, and the TMD/CT alone is sufficient to direct the GFP protein to both organelles.

To confirm the subcellular localization of AtPAP2, protein extracts from isolated chloroplasts and mitochondria were probed with the antibody against AtPAP2. A protein band with an apparent molecular mass of 74 kD was detected in both mitochondria and chloroplasts. The purity of the mitochondria and chloroplasts was verified using antibodies raised against a variety of mitochondrial and chloroplast specific proteins (Fig. 2j).

C-terminal targeting is crucial for AtPAP2 function

To further study the function of the C-terminal motif and the putative signal peptide of AtPAP2, OE lines with AtPAP2 truncation of the C-terminal motif (a.a. 588–656) or its predicted SP (a.a. 1–24) were generated in *Arabidopsis* by Agrobacterium-mediated plant transformation (Fig. 3). Western blot analysis was employed to verify its overexpression in homozygous transgenic lines.

As shown in Fig. 3(a), transgenic *Arabidopsis* lines expressing SP-deleted AtPAP2 (P2NS, a.a. 25–656) exhibited phenotypes similar to the full-length AtPAP2 OE lines, such as earlier bolting and higher biomass. By contrast, when the C-terminal motif was deleted, the OE lines (P2NC, a.a. 1–588) grew like the WT *Arabidopsis* (Fig. 3a). These results suggest that the C-terminal motif of AtPAP2 is critical for its function in *Arabidopsis*. By contrast, the putative N-terminal signal peptide of AtPAP2 does not seem to be essential.

In AtPAP2 OE lines (P2OE and P2NS), two protein bands could be seen in membrane fractions but only the low molecular weight band appeared in the soluble fraction. Furthermore, the high molecular weight protein band was not seen in the membrane fraction from the P2NC lines (with no C-terminal motif). Therefore, it is likely that the high molecular weight protein band is a membrane-associated full-length AtPAP2 and the cleavage of its C-terminal motif releases it to the soluble fraction. Correlated with the growth phenotype, the presence of the membrane-associated high molecular weight form is essential to the robust growth phenotypes of the OE lines (Fig. 3b).

AtPAP2 overexpression changes the C metabolism of *Arabidopsis*

Sugars supplied by the shoot are the driving force for plant growth and anabolism. We analyzed the carbohydrate contents of leaves from 20-d-old plants halfway through the light period. The size and morphology of leaves from various lines were still similar at day 20 and therefore this age was chosen for further analysis. Both sucrose and hexose sugar contents were greatly elevated in the shoots of AtPAP2 OE plants (Table 1c), in which sucrose was 1.3- to 1.8-fold and hexose sugars were 1.9- to 2.6-fold that of WT ($P < 0.01$). However, the starch level did not differ significantly between the various lines (Table 1c).

The increased sucrose and hexose sugars (Table 1c) in the AtPAP2 OE plants may be due to altered activity of enzymes involved in sugar metabolism. SPS activity was significantly enhanced in the 20-d-old AtPAP2 OE lines under both optimal V_{max} and limiting V_{limit} conditions, and was not affected by light/dark transitions, as in WT *Arabidopsis* (Huber *et al.*, 1989). In addition, the activities of enzymes involved in sucrose catabolism, including sucrose synthase, acid and alkaline soluble invertase, insoluble cell wall invertases, were unaffected (Table 2). The enzyme activity of acid phosphatase was elevated in both OE lines but the total NR activity was only significantly elevated in one OE line (OE21, Table 2). The higher SPS activity could result from either a higher level of protein expression or

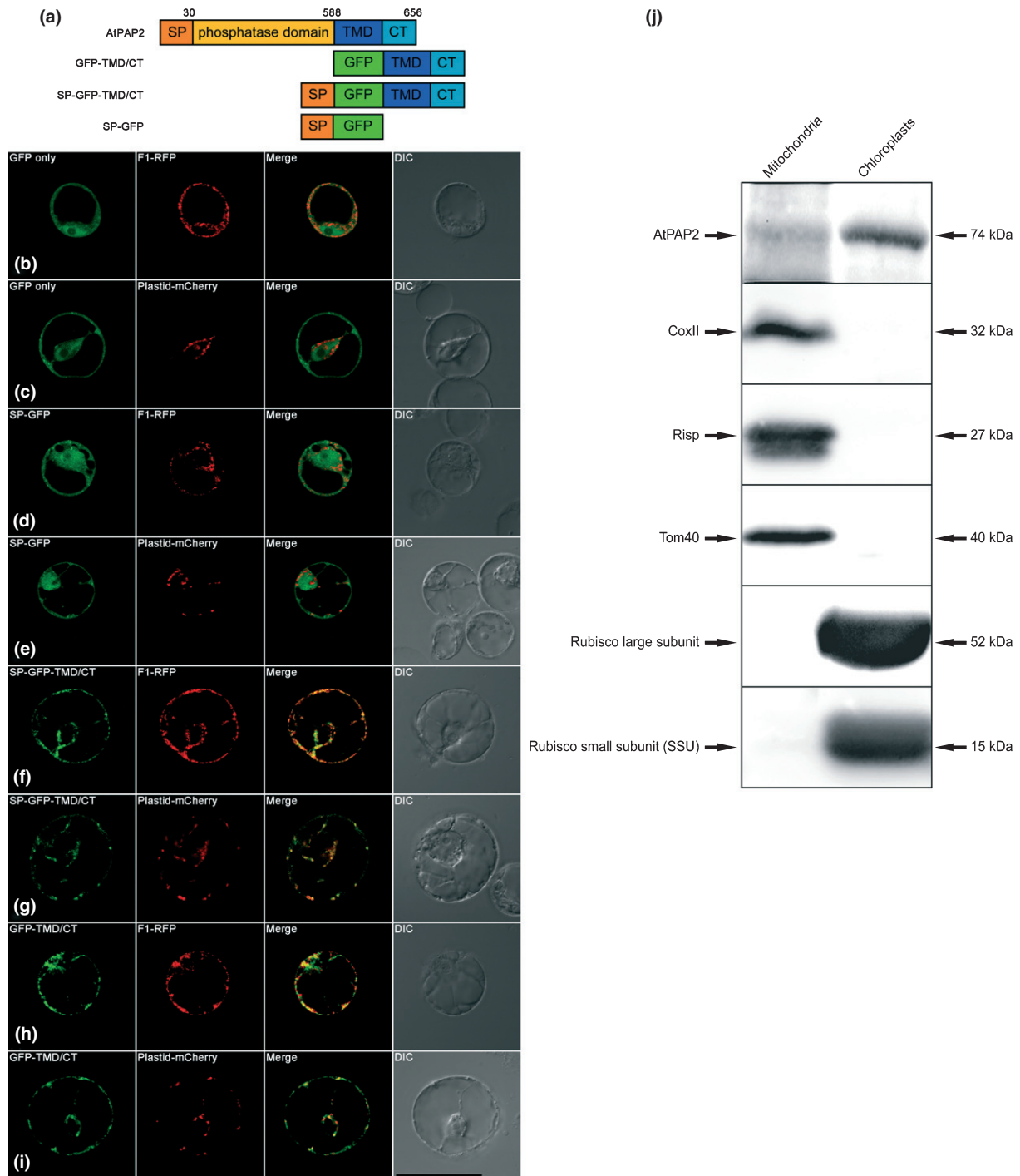


Fig. 2 AtPAP2 protein is targeted to both mitochondria and chloroplasts. (a) Targeting of GFP fusion proteins in Arabidopsis PSB-D protoplasts. Transient expression in Arabidopsis PSB-D protoplasts showed that GFP (GFP only) (b, c) and GFP fused with the putative SP region of AtPAP2 (SP-GFP) (d, e) were directed to the cytosol, whereas GFP constructs fused with the TMD/CT region of AtPAP2, including SP-GFP-TMD/CT (f, g) and GFP-TMD/CT (h, i), co-localized with mitochondrial (F1-RFP) and chloroplastic (plastid-mCherry) markers. Bar, 50 μ m. Western blot of AtPAP2 protein in mitochondria and chloroplasts. (j) Isolated mitochondria and chloroplasts from 10-d-old seedlings were analyzed by western blotting for the presence of AtPAP2. Purity of the isolated organelles was determined by blotting with antibodies specific to each organelle. Mitochondria, cytochrome oxidase subunit II (CoxII), the Rieske iron sulfur cluster binding protein (Risp) and translocase of the outer membrane protein of 40 kDa (Tom40); chloroplasts, Rubisco large subunit and Rubisco small subunit (SSU).

a higher activity per enzyme molecule. Western blotting indicated that the SPS protein levels were significantly elevated in the OE lines during both day and night. The levels of the other

enzymes, such as fructose-1,6-bisphosphatase (FBPase) and FBP aldolase in the sucrose synthetic pathway did not change significantly (Fig. 4).

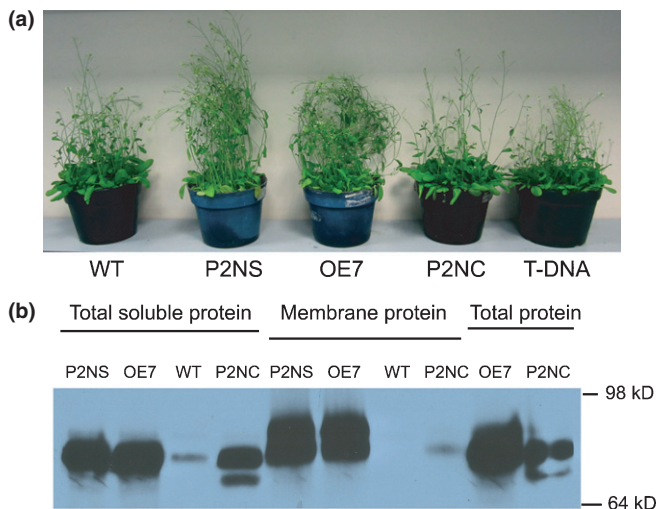


Fig. 3 AtPAP2 sublocalization in transgenic plants. (a) Phenotype of 40-d-old plants ($n = 12$) of wild-type (WT), P2NS (a.a. 25–656), OE7 (a.a. 1–656), P2NC (a.a. 1–588) and *AtPAP2* T-DNA Arabidopsis plants. (b) AtPAP2 protein band identification in WT, P2NS, OE7, P2NC and *AtPAP2* T-DNA plants by western blot analysis.

To investigate whether enhanced SPS activity was due to a change in the relative amounts of phosphorylated SPS vs total SPS, a 14-3-3 capture experiment was carried out. The recombinant 14-3-3 captured similar amounts of phosphorylated SPS in all four lines (Fig. 4). Hence, the increase in SPS activity in the OE lines was due to an increase of the unphosphorylated active form of enzyme. Theoretically, a suppression of SnRK1 kinase

activity could enhance SPS activity. Hence, the expression levels of SnRK1 protein subunits and the phosphorylation status of the Thr₁₇₅ residue on its activation loop were examined by western blotting (Fig. S10); the levels of the AtSnRK1.1, AtSnRK β 1 and AtSnRK β 2 subunits were unaltered. Blots using antiserum against phosphorylated-AMPK (T₁₇₂), which cross-reacts with phosphorylated Thr₁₇₅ on AtSnRK1 in Arabidopsis (Sugden *et al.*, 1999), indicated that the phosphorylation status of T₁₇₅ was unaltered. This suggested that the higher SPS activity in the OE lines was not mediated by the SnRK1 pathway.

Overexpression of *AtPAP2* results in alteration of soluble plastid proteins

Two-dimensional gel analysis of total leaf soluble proteins revealed that two proteins involved in photosynthesis exhibited changes in the OE lines; first, PSBP-1, an oxygen-evolving enhancer protein (AT1G06680), was induced, and second, Rubisco activase (RCA, AT2G39730) showed a mobility shift (Fig. 5). PSBP-1 is required for high levels of oxygen evolution (Mayfield *et al.*, 1987). RCA enhances photosynthetic rate by freeing Rubisco for the next round of C fixation (Portis, 2003; Portis *et al.*, 2008). In Arabidopsis, there are two RCA genes (At1g73110 and At2g39730), and alternative splicing of At2g39730 produced three isoforms. Deletion of the short thermolabile isoform of At2g39730 (RCA1) caused decreased seed yield while transgenic Arabidopsis overexpressing thermostable RCA1 exhibited higher biomass and photosynthetic rate (Kurek *et al.*, 2007). According to the PhosphAT database

Table 2 Enzyme assays: samples were collected 8 h after the light period (Day) and 4 h after the dark period (Night)

Plant line	WT	T-DNA	OE7	OE21
Sucrose phosphate synthase ($\mu\text{mol sucrose mg}^{-1}$ total soluble protein h^{-1})				
V_{max} (Day)	5.44 \pm 0.90 ^a	5.80 \pm 0.59 ^a	7.89 \pm 1.08 ^b	7.97 \pm 0.95 ^b
V_{limit} (Day)	3.18 \pm 0.32 ^a	3.47 \pm 0.12 ^a	4.54 \pm 0.92 ^b	3.99 \pm 0.68 ^a
V_{max} (Night)	5.91 \pm 0.57 ^a	5.24 \pm 0.72 ^a	7.54 \pm 0.97 ^b	6.82 \pm 0.75 ^a
V_{limit} (Night)	3.74 \pm 0.31 ^a	2.83 \pm 0.16 ^b	4.67 \pm 0.18 ^c	4.86 \pm 0.54 ^c
Sucrose synthase ($\mu\text{mol glucose mg}^{-1}$ total soluble protein h^{-1})				
Day	12.46 \pm 0.23 ^a	12.35 \pm 1.20 ^a	12.43 \pm 0.22 ^a	12.76 \pm 0.27 ^a
Night	12.47 \pm 0.36 ^a	12.63 \pm 0.44 ^a	12.54 \pm 0.43 ^a	12.94 \pm 0.27 ^a
Soluble invertase ($\mu\text{mol glucose mg}^{-1}$ total soluble protein h^{-1})				
Day (Acid)	0.71 \pm 0.11 ^a	0.60 \pm 0.27 ^a	0.91 \pm 0.45 ^a	0.90 \pm 0.04 ^a
Night (Acid)	0.70 \pm 0.34 ^a	1.30 \pm 0.5 ^a	0.88 \pm 0.21 ^a	0.69 \pm 0.04 ^a
Day (Alkaline)	8.48 \pm 0.49 ^a	8.06 \pm 1.61 ^a	8.04 \pm 1.39 ^a	8.94 \pm 0.84 ^a
Night (Alkaline)	6.50 \pm 0.41 ^a	5.25 \pm 0.63 ^a	6.80 \pm 0.68 ^a	6.83 \pm 0.07 ^a
Insoluble cell wall invertase ($\mu\text{mol sucrose mg}^{-1}$ total soluble protein h^{-1})				
Day (Acid)	1.11 \pm 0.19 ^a	0.90 \pm 0.24 ^a	1.17 \pm 0.31 ^a	1.20 \pm 0.33 ^a
Night (Acid)	1.08 \pm 0.50 ^a	0.85 \pm 0.21 ^a	1.41 \pm 0.21 ^a	1.11 \pm 0.16 ^a
Day (Alkaline)	6.08 \pm 0.14 ^a	6.35 \pm 0.11 ^a	5.09 \pm 0.32 ^a	5.27 \pm 0.10 ^a
Night (Alkaline)	6.94 \pm 0.31 ^a	7.57 \pm 0.43 ^a	6.17 \pm 0.28 ^a	6.77 \pm 0.73 ^a
Nitrate reductase ($\mu\text{mol nitrite g}^{-1}$ FW h^{-1})				
Middle of the day	0.14 \pm 0.00 ^a	0.15 \pm 0.01 ^a	0.17 \pm 0.00 ^a	0.24 \pm 0.02 ^b
Middle of the night	0.13 \pm 0.01 ^a	0.13 \pm 0.05 ^a	0.15 \pm 0.04 ^{ab}	0.20 \pm 0.01 ^c
Acid phosphatase activity ($\mu\text{mol Pi mg}^{-1}$ total soluble protein h^{-1})				
Middle of the day	8.33 \pm 1.38 ^a	8.05 \pm 1.14 ^a	18.46 \pm 1.91 ^b	16.59 \pm 1.04 ^b
Middle of the night	6.04 \pm 0.11 ^a	6.00 \pm 0.81 ^a	10.71 \pm 0.12 ^b	13.71 \pm 0.56 ^c

Values marked with a different letter were determined by the *t* test to be significantly different from wild-type (WT) and were determined by the ANOVA–Tukey test to be significantly different ($P < 0.05$) from each other. There are three biological replicates in this study.

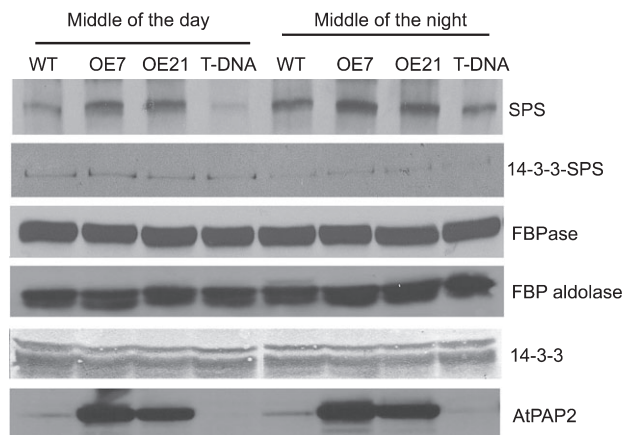


Fig. 4 Western blotting of enzymes involved in sucrose biosynthesis. Total soluble protein (30 μ g) extracted from the shoots of 20-d-old Arabidopsis plants was loaded to each lane and was analyzed by western blotting using anti-SPS, anti-FBP aldolase and anti-cFBPase antibodies (Agriser). The pulled-down eluates of GST-14-3-3 were diluted 1 : 1 with 40 μ l SDS sample buffer and half was loaded into each lane.

(phosphat.mpimp-golm.mpg.de), there is at least one phosphorylation site in both gene products (GLAYDpTSDDQ on At2G39730.1; AGGMEpTLGKV and VPLIVpTGNDF on AT1G73110.1). A change in phosphorylation status of RCA conceivably would affect pI, but whether this occurred was not determined.

Metabolomic analysis

Metabolomic analysis was carried out using a combination of NMR-MS and GC-MS. Shoot samples were collected from 20-d-old plants before bolting. Principal component analysis of $^1\text{H-NMR}$ and GS-MS datasets (Fig. S11) was carried out to discern any global changes in the metabolomes of these lines. There was a very clear separation of the OE lines from WT and the T-DNA insertion line by each analytical technique. $^1\text{H-NMR}$ was also able to discriminate the T-DNA line from WT samples, although this separation was much smaller. The main changes that could be discerned by $^1\text{H-NMR}$ between the T-DNA samples and WT included a reduction in fumarate and citrate levels and several amino acids.

Combining the results of metabolomics analysis and LC-MS-MS measurements, metabolites which were increased in the OE

lines included alanine, proline, several tricarboxylic acid (TCA) metabolites (citrate, fumarate, malate), sugars (glucose and sucrose) and a metabolite putatively identified as indole acetonitrile, a breakdown product of indole glucosinolate. Reduced metabolites in the OE lines included certain amino acids (asparagine, aspartate, glutamine, lysine, methionine, phenylalanine, threonine, tyrosine), GABA, ethanolamine, 4-hydroxybenzoic acid, ribose, phytol, linoleic acid, and linolenic acid (Table S2). In addition, OE lines contained significantly higher levels of putrescine and significantly lower levels of spermidine. The metabolites detected in the glycolysis, TCA and amino acid synthesis pathways are presented in Fig. 6.

Discussion

The genomes of plant species generally contain multiple PAP-like sequences, among which, except Arabidopsis, usually only a single PAP gene carries a C-terminal hydrophobic motif. Amino acid sequence alignment of the 29 PAP-like sequences from the Arabidopsis genome showed that only two AtPAPs (AtPAP2, AT1G13900 and AtPAP9, AT2G03450) carry an additional hydrophobic motif (a.a. 614–636 of AtPAP2 and a.a. 604–626 of AtPAP9) at their C-termini (Table S1), which was predicted as a trans-membrane motif by the TMHMM program. Although AtPAP9 shares up to 72% sequence identity with AtPAP2 at protein level, AtPAP9 did not exhibit the biological function of AtPAP2. A homozygous T-DNA line of *AtPAP9* (Salk_129905) and several homozygous *AtPAP9* OE lines were identified by genomic PCR and RT-PCR analysis. All of them exhibited normal growth phenotypes, which were very different from that of *AtPAP2* OE lines (data not shown). A double T-DNA insertion line of *AtPAP2* and *AtPAP9* was also generated through crossing the pollens of *AtPAP2* insertion line and the pistil of *AtPAP9* insertion line and the interruption of both genes were confirmed by genomic PCR analysis (Fig. S3). The double insertion line exhibited similar phenotypes with that of the *AtPAP2* T-DNA line (data not shown). In addition, two PAP-like sequences could be identified in the genomes of the small free-living photosynthetic eukaryotes *O. tauri* (Derelle *et al.*, 2006) and *Micromonas pusilla* (Worden *et al.*, 2009), of which only one carries a hydrophobic C-terminal motif. *O. tauri*, belonging to the Prasinophyceae, is the smallest (size < 1 μm) free-living photosynthetic eukaryote known. This unicellular organism lacks

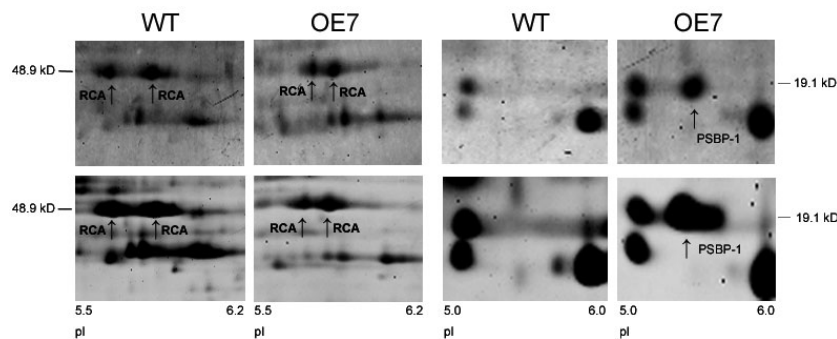


Fig. 5 Analysis of protein from *AtPAP2* overexpression (OE) lines. An equal volume of total soluble protein (300 μ g) extracted from 20-d-old Arabidopsis plants was analyzed by 2-D gel electrophoresis. Gels were stained with Pro-Q Diamond and SYPRO Ruby. The pI range of the gel was 4–7. Targeted spots are identified by the arrows. Mobility shifts of Rubisco activase (RCA) and oxygen-evolving enhancer protein (PSBP-1) are indicated by the arrows. Three biological replicates were used in this study.

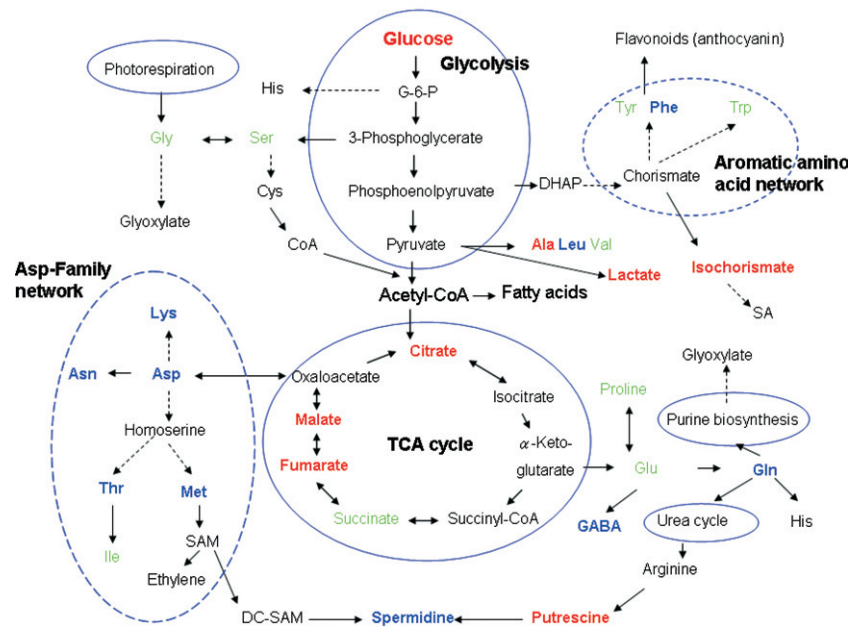


Fig. 6 Altered metabolites in 20-d-old AtPAP2 overexpression (OE) lines. Metabolites in red and blue indicate increased or decreased levels, respectively, in AtPAP2 OE plants. Metabolites in black were not detected and those in green were unaltered. The dashed blue circles represent the Asp-family and aromatic amino acid network. DHAP, dihydroxyacetone phosphate; GABA, γ -aminobutyric acid; SA, salicylic acid; DC-SAM, decarboxylated S-adenosylmethionine; TCA, tricarboxylic acid.

a cell wall and each cell carries one chloroplast, one mitochondrion, one Golgi body and a large nucleus. The Prasinophyceae are a primitive group of marine green algae, which suggests an ancient ancestral function of AtPAP2-like proteins in the regulation of C partitioning in photosynthetic organisms.

In our study, AtPAP2 was shown to be dual-targeted to both chloroplasts and mitochondria, key organelles for two important energy processes in plant cells: photosynthesis and respiration (Nunes-Nesi *et al.*, 2007, 2011). An increasing number of proteins in mitochondria and plastids have been found to be encoded by single nuclear genes, and are referred to as dual-targeted proteins (Peeters & Small, 2001). To date, as many as 47 different proteins from seven plant species have been reported to be dual-targeted (Carrie *et al.*, 2009a). In Arabidopsis, 11 PKs and 10 PPs have been shown to be targeted to the chloroplast and all are nuclear encoded (Schliebner *et al.*, 2008; Shapiguzov *et al.*, 2010). In mitochondria, 10 PKs and one PP were identified in Arabidopsis (Heazlewood *et al.*, 2004). All of these PKs and PPs are targeted by N-terminal targeting signals. The identification of a C-terminal dual-targeting signal in AtPAP2 is novel and AtPAP2 is the only PP that is dual-targeted to both organelles.

Overexpression of AtPAP2 in Arabidopsis leads to a faster growth rate. The higher biomass but lower total leaf area of 40-d-old transgenic plants provided indirect evidence of a higher photoassimilation rate per leaf area in the OE lines. The changes in RCA and PSBP-1 in the OE lines might also affect the photosynthetic activity of the OE lines. Whether the observed modification of RCA affects the activity of Rubisco and thus results in the enhanced growth rate of AtPAP2 OE lines is an interesting topic for further study.

Sucrose is the fuel and building block for sink tissues. AtPAP2 overexpression drastically enhanced the sucrose and hexose levels in rosette leaves while the starch level did not change significantly. SPS activity shows a high correlation with sucrose

production in leaves (Baxter *et al.*, 2003; Haigler *et al.*, 2007) and overexpression of SPS promotes earlier flowering, fruit development, and increased biomass in tomato (Micallef *et al.*, 1995) and tobacco (Park *et al.*, 2008). In the two AtPAP2 OE lines, SPS was upregulated at the protein level, which resulted in a significant enhancement of its activity. SnRK1 can phosphorylate and inhibit SPS activity (Halford *et al.*, 2003) under high sucrose levels. Since overexpression of AtSnRK1.1 resulted in phenotypes opposite to that of the AtPAP2 OE plants, such as delayed flowering and retarded growth (Baena-Gonzalez *et al.*, 2007), it may be worth asking whether AtPAP2 is an antagonistic phosphatase of SnRK's kinase activity. Under energy deficiency, activated SnRK1 phosphorylates SPS hence suppresses activity posttranslationally (Toroser *et al.*, 1998; Moorhead *et al.*, 1999). By contrast, overexpression of AtPAP2 resulted in higher SPS activity. Theoretically, a phosphatase (Sugden *et al.*, 1999) that specifically dephosphorylates SnRK1 or its upstream kinases (e.g. GRIK) *in vivo* might suppress their biological activity and thus boost the activity of SPS. However, it is unlikely that AtPAP2 mediated its actions through GRIK or SnRK1 because the phosphorylation status of the T₁₇₅ residue was unaltered in the OE lines; also, pull-down experiments only found an interaction between GRIK and SnRK (data not shown), but not between AtPAP2 and GRIK or SnRK1 (Fig. S10). Unlike SnRK1, which inactivates SPS by posttranslational modification, AtPAP2 overexpression enhances sucrose synthesis by increasing the expression of SPS.

The mechanism of how AtPAP2 stimulates plant growth remains unclear. As the acid phosphatase activity was significantly increased in the AtPAP2 OE lines (Table 2), AtPAP2 may act as a PP or as a phosphatase for inorganic P compounds. In the former scenario, AtPAP2 might exhibit its effects as a PP like PPH1, a chloroplast phosphatase that dephosphorylates light-harvesting complex II during state transition (Finazzi *et al.*, 2002; Shapiguzov *et al.*, 2010). In the latter scenario, AtPAP2

might increase the acid phosphatase activity in the chloroplasts and mitochondria, thus releasing more free inorganic phosphate (Pi). In chloroplasts, as Pi is an activator of Rubisco activity, production of triose phosphates might be enhanced by a higher Pi supply (Giersch & Robinson, 1987), and in turn provide more triose phosphate for sucrose synthesis. Similarly, the possibly higher Pi supply in the mitochondrial matrix could also modulate TCA flux and activate oxidative phosphorylation and ATP synthesis (Wu *et al.*, 2007). The higher concentrations of fumarate and malate in OE lines (Fig. 6) might reflect a higher flux from succinyl-CoA to succinate (Johnson *et al.*, 1998), another step in the TCA cycle that produces ATP (Meyer *et al.*, 2010). ATP generated from the TCA cycle could be transported out of the mitochondria to sustain the high rate of sucrose synthesis (Krömer *et al.*, 1993). The higher levels of organic acids of the TCA cycle in the OE lines did not result in a higher amino acid level of the aspartate family, indicating that the regulation and the flux of the TCA cycle is a complicated process. Alteration of key enzymes and their activities in the TCA cycle affect photosynthesis: downregulation of aconitase, the iron-sulfur subunit of succinate dehydrogenase and the mitochondrial malate dehydrogenase enhance the rate of photosynthesis (Carrari *et al.*, 2003; Nunes-Nesi *et al.*, 2005; Araujo *et al.*, 2011), whereas inhibition of citrate synthase, succinyl CoA ligase, or isocitrate dehydrogenase show little effect on the rate (Studart-Guimaraes *et al.*, 2007; Sienkiewicz-Porzucek *et al.*, 2008, 2010; Sulpice *et al.*, 2010). All these lines displayed changes in expression levels of organic acids and amino acids. Thus, the mechanism by which AtPAP2 influences both photosynthesis and the TCA cycle is likely to be complex and may be involved in a number of pathways or factors.

In summary, we have shown that ectopic overexpression of AtPAP2 in *Arabidopsis* causes dramatic effects on plant growth and C metabolism. Its biological activity is dependent on its dual targeting to both plastids and mitochondria. Whether overexpression of AtPAP can be used as a tool to boost the yield of important crop plants will be an interesting subject of future studies.

Acknowledgements

This project was supported by the General Research Fund (HKU772710M) and the Innovation and Technology Fund (ITS158/09) of the HKSAR, China. We thank Dr Yip's lab at HKU for kindly providing plant vectors and technical support for plant cultures. We thank Aimee Llewellyn and Delia Corol at Rothamsted Research for preparation of the analytical extracts and for ¹H-NMR data collection, Dr David Secco at the University of Western Australia for his comments on this manuscript.

References

- Antonio C, Larson T, Gilday A, Graham I, Bergstrom E, Thomas-Oates J. 2007. Quantification of sugars and sugar phosphates in *Arabidopsis thaliana* tissues using porous graphitic carbon liquid chromatography-electrospray ionization mass spectrometry. *Journal of Chromatography A* 1172: 170–178.
- Antonio C, Larson T, Gilday A, Graham I, Bergstrom E, Thomas-Oates J. 2008. Hydrophilic interaction chromatography/electrospray mass spectrometry analysis of carbohydrate-related metabolites from *Arabidopsis thaliana* leaf tissue. *Rapid Communications in Mass Spectrometry* 22: 1399–1407.
- Araujo WL, Nunes-Nesi A, Osorio S, Usadel B, Fuentes D, Nagy R, Balbo I, Lehmann M, Studart-Witkowski C, Tohge T *et al.* 2011. Antisense inhibition of the iron-sulfur subunit of succinate dehydrogenase enhances photosynthesis and growth in tomato via an organic acid-mediated effect on stomatal aperture. *Plant Cell* 23: 600–627.
- Baena-Gonzalez E, Rolland F, Thevelein JM, Sheen J. 2007. A central integrator of transcription networks in plant stress and energy signalling. *Nature* 448: 938–942.
- Baxter CJ, Foyer CH, Turner J, Rolfe SA, Quick WP. 2003. Elevated sucrose-phosphate synthase activity in transgenic tobacco sustains photosynthesis in older leaves and alters development. *Journal of Experimental Botany* 54: 1813–1820.
- Beale MH, Ward JL, Baker JM, Miller SJ, Deborde C, Maucourt M, Biais B, Rolin D, Moing A, Moco S *et al.* 2010. An inter-laboratory comparison demonstrates that [(1)H]-NMR metabolite fingerprinting is a robust technique for collaborative plant metabolomic data collection. *Metabolomics* 6: 263–273.
- Cai Y, Jia TR, Lam SK, Ding Y, Gao CJ, San MWY, Pimpl P, Jiang LW. 2011. Multiple cytosolic and transmembrane determinants are required for the trafficking of SCAMP1 via an ER-Golgi-TGN-PM pathway. *Plant Journal* 65: 882–896.
- Carrari F, Nunes-Nesi A, Gibon Y, Lytovchenko A, Loureiro ME, Fernie AR. 2003. Reduced expression of aconitase results in an enhanced rate of photosynthesis and marked shifts in carbon partitioning in illuminated leaves of wild species tomato. *Plant Physiology* 133: 1322–1335.
- Carrie C, Giraud E, Duncan O, Xu L, Wang Y, Huang SB, Clifton R, Murcha M, Filipovska A, Rackham O *et al.* 2010. Conserved and novel functions for *Arabidopsis thaliana* MIA40 in assembly of proteins in mitochondria and peroxisomes. *Journal of Biological Chemistry* 285: 36138–36148.
- Carrie C, Giraud E, Whelan J. 2009a. Protein transport in organelles: dual targeting of proteins to mitochondria and chloroplasts. *The FEBS Journal* 276: 1187–1195.
- Carrie C, Kuhn K, Murcha MW, Duncan O, Small ID, O'Toole N, Whelan J. 2009b. Approaches to defining dual-targeted proteins in *Arabidopsis*. *The Plant Journal: For Cell and Molecular Biology* 57: 1128–1139.
- Carrie C, Murcha MW, Kuehn K, Duncan O, Barthet M, Smith PM, Eubel H, Meyer E, Day DA, Millar AH *et al.* 2008. Type II NAD(P)H dehydrogenases are targeted to mitochondria and chloroplasts or peroxisomes in *Arabidopsis thaliana*. *FEBS Letters* 582: 3073–3079.
- Cashikar AG, Kumaresan R, Rao NM. 1997. Biochemical characterization and subcellular localization of the red kidney bean purple acid phosphatase. *Plant Physiology* 114: 907–915.
- Chen S, Songkumarn P, Liu J, Wang GL. 2009. A versatile zero background T-vector system for gene cloning and functional genomics. *Plant Physiology* 150: 1111–1121.
- Ciereszko I, Johansson H, Kleczkowski L. 2001. Sucrose and light regulation of a cold-inducible UDP-glucose pyrophosphorylase gene via a hexokinase-independent and abscisic acid-insensitive pathway in *Arabidopsis*. *Biochemical Journal* 354: 67.
- Clough SJ, Bent AF. 1998. Floral dip: a simplified method for *Agrobacterium*-mediated transformation of *Arabidopsis thaliana*. *Plant Journal* 16: 735–743.
- Dabney-Smith C, van den Wijngaard PWJ, Treece Y, Vredenberg WJ, Bruce BD. 1999. The C terminus of a chloroplast precursor modulates its interaction with the translocation apparatus and PIRAC. *Journal of Biological Chemistry* 274: 32351–32359.
- De Caroli M, Lenucci MS, Di Sansebastiano GP, Dalessandro G, De Lorenzo G, Piro G. 2011. Protein trafficking to the cell wall occurs through mechanisms distinguishable from default sorting in tobacco. *Plant Journal* 65: 295–308.
- Dejardin A, Rochat C, Maugenest S, Boutin JP. 1997. Purification, characterization and physiological role of sucrose synthase in the pea seed coat (*Pisum sativum* L.). *Planta* 201: 128–137.

- Derelle E, Ferraz C, Rombauts S, Rouze P, Worden AZ, Robbens S, Partensky F, Degroevae S, Echeynie S, Cooke R *et al.* 2006. Genome analysis of the smallest free-living eukaryote *Ostreococcus tauri* unveils many unique features. *Proceedings of the National Academy of Sciences, USA* 103: 11647–11652.
- Duby G, Oufattole M, Boutry M. 2001. Hydrophobic residues within the predicted N-terminal amphiphilic alpha-helix of a plant mitochondrial targeting presequence play a major role in *in vivo* import. *Plant Journal* 27: 539–549.
- Finazzi G, Rappaport F, Furia A, Fleischmann M, Rochaix JD, Zito F, Forti G. 2002. Involvement of state transitions in the switch between linear and cyclic electron flow in *Chlamydomonas reinhardtii*. *EMBO Reports* 3: 280–285.
- Focks N, Benning C. 1998. wrinkled1: a novel, low-seed-oil mutant of *Arabidopsis* with a deficiency in the seed-specific regulation of carbohydrate metabolism. *Plant Physiology* 118: 91–101.
- Gibson SI. 2005. Control of plant development and gene expression by sugar signaling. *Current Opinion in Plant Biology* 8: 93–102.
- Giersch C, Robinson SP. 1987. Regulation of photosynthetic carbon metabolism during phosphate limitation of photosynthesis in isolated spinach chloroplasts. *Photosynthesis Research* 14: 211–227.
- Haigler CH, Singh B, Zhang DS, Hwang S, Wu CF, Cai WX, Hozain M, Kang W, Kiedaisch B, Strauss RE *et al.* 2007. Transgenic cotton over-producing spinach sucrose phosphate synthase showed enhanced leaf sucrose synthesis and improved fiber quality under controlled environmental conditions. *Plant Molecular Biology* 63: 815–832.
- Halford NG, Hey S, Jhurreea D, Laurie S, McKibbin RS, Paul M, Zhang YH. 2003. Metabolic signalling and carbon partitioning: role of Snf1-related (SnRK1) protein kinase. *Journal of Experimental Botany* 54: 467–475.
- Heazlewood JL, Tonti-Filippini JS, Gout AM, Day DA, Whelan J, Millar AH. 2004. Experimental analysis of the *Arabidopsis* mitochondrial proteome highlights signaling and regulatory components, provides assessment of targeting prediction programs, and indicates plant-specific mitochondrial proteins. *Plant Cell* 16: 241–256.
- Huber SC, Huber JL, Campbell WH, Redinbaugh MG. 1992. Apparent dependence of the light activation of nitrate reductase and sucrose phosphate synthase activities in spinach leaves on protein synthesis. *Plant and Cell Physiology* 33: 639–646.
- Huber SC, Nielsen TH, Huber JLA, Pharr DM. 1989. Variation among species in light activation of sucrose-phosphate synthase. *Plant and Cell Physiology* 30: 277–285.
- Johnson JD, Mehus JG, Tews K, Milavetz BI, Lambeth DO. 1998. Genetic evidence for the expression of ATP- and GTP-specific succinyl-CoA synthetases in multicellular eucaryotes. *Journal of Biological Chemistry* 273: 27580–27586.
- Kaida R, Satoh Y, Bulone V, Yamada Y, Kaku T, Hayashi T, Kaneko TS. 2009. Activation of β -glucan synthases by wall bound purple acid phosphatase in tobacco cells. *Plant Physiology* 150: 1822–1830.
- Kaida R, Serada S, Norioka N, Norioka S, Neumetzler L, Pauly M, Sampedro J, Zarra I, Hayashi T, Kaneko TS. 2010. Potential role for purple acid phosphatase in the dephosphorylation of wall proteins in tobacco cells. *Plant Physiology* 153: 603–610.
- Kleffmann T, Russenberger D, von Zychlinski A, Christopher W, Sjolander K, Gruissem W, Baginsky S. 2004. The *Arabidopsis thaliana* chloroplast proteome reveals pathway abundance and novel protein functions. *Current Biology* 14: 354–362.
- Krömer S, Malmberg G, Gardestrom P. 1993. Mitochondrial contribution to photosynthetic metabolism: a study with barley (*Hordeum vulgare* L.) leaf protoplasts at different light intensities and CO₂ concentrations. *Plant Physiology* 102: 947–955.
- Kuang R, Chan KH, Yeung E, Lim BL. 2009. Molecular and biochemical characterization of AtPAP15, a purple acid phosphatase with phytase activity, in *Arabidopsis*. *Plant Physiology* 151: 199–209.
- Kubis SE, Lilley KS, Jarvis P. 2008. Isolation and preparation of chloroplasts from *Arabidopsis thaliana* plants. *Methods in Molecular Biology* 425: 171–186.
- Kumar S, Tamura K, Nei M. 2004. MEGA3: integrated software for molecular evolutionary genetics analysis and sequence alignment. *Briefings in Bioinformatics* 5: 150–163.
- Kurek I, Chang TK, Bertain SM, Madrigal A, Liu L, Lassner MW, Zhu G. 2007. Enhanced thermostability of *Arabidopsis* Rubisco activase improves photosynthesis and growth rates under moderate heat stress. *Plant Cell* 19: 3230–3241.
- Li D, Zhu H, Liu K, Liu X, Leggewie G, Udvardi M, Wang D. 2002. Purple acid phosphatases of *Arabidopsis thaliana*. Comparative analysis and differential regulation by phosphate deprivation. *Journal of Biological Chemistry* 277: 27772–27781.
- Li W-YF, Shao G, Lam H-M. 2008. Ectopic expression of *GmPAP3* alleviates oxidative damage caused by salinity and osmotic stresses. *New Phytologist* 178: 80–91.
- Liao H, Wong FL, Phang TH, Cheung MY, Li WY, Shao G, Yan X, Lam HM. 2003. *GmPAP3*, a novel purple acid phosphatase-like gene in soybean induced by NaCl stress but not phosphorus deficiency. *Gene* 318: 103–111.
- Lister R, Carrie C, Duncan O, Ho LH, Howell KA, Murcha MW, Whelan J. 2007. Functional definition of outer membrane proteins involved in preprotein import into mitochondria. *The Plant cell* 19: 3739–3759.
- Lung SC, Leung A, Kuang R, Wang Y, Leung P, Lim BL. 2008. Phytase activity in tobacco (*Nicotiana tabacum*) root exudates is exhibited by a purple acid phosphatase. *Phytochemistry* 69: 365–373.
- Lunn JE, Furbank RT. 1997. Localisation of sucrose-phosphate synthase and starch in leaves of C₄ plants. *Planta* 202: 106–111.
- Lunn JE, MacRae E. 2003. New complexities in the synthesis of sucrose. *Current Opinion in Plant Biology* 6: 208–214.
- Martinez-Noel GM, Tognetti JA, Salerno GL, Wiemken A, Pontis HG. 2009. Protein phosphatase activity and sucrose-mediated induction of fructan synthesis in wheat. *Planta* 230: 1071–1079.
- Mayfield SP, Rahire M, Frank G, Zuber H, Rochaix JD. 1987. Expression of the nuclear gene encoding oxygen-evolving enhancer protein 2 is required for high levels of photosynthetic oxygen evolution in *Chlamydomonas reinhardtii*. *Proceedings of the National Academy of Sciences, USA* 84: 749–753.
- Meyer S, De Angeli A, Fernie AR, Martinoia E. 2010. Intra- and extra-cellular excretion of carboxylates. *Trends in Plant Science* 15: 40–47.
- Miao Y, Jiang L. 2007. Transient expression of fluorescent fusion proteins in protoplasts of suspension cultured cells. *Nature Protocols* 2: 2348–2353.
- Micallef B, Haskins K, Vanderveer P, Roh K, Shewmaker C, Sharkey T. 1995. Altered photosynthesis, flowering, and fruiting in transgenic tomato plants that have an increased capacity for sucrose synthesis. *Planta* 196: 327–334.
- Moorhead G, Douglas P, Cotelle V, Harthill J, Morrice N, Meek S, Deiting U, Stitt M, Scarabel M, Aitken A *et al.* 1999. Phosphorylation-dependent interactions between enzymes of plant metabolism and 14-3-3 proteins. *Plant Journal* 18: 1–12.
- Nelson BK, Cai X, Nebenfuhr A. 2007. A multicolored set of *in vivo* organelle markers for co-localization studies in *Arabidopsis* and other plants. *Plant Journal* 51: 1126–1136.
- Nunes-Nesi A, Araujo WL, Fernie AR. 2011. Targeting mitochondrial metabolism and machinery as a means to enhance photosynthesis. *Plant Physiology* 155: 101–107.
- Nunes-Nesi A, Carrari F, Lytovchenko A, Smith AMO, Loureiro ME, Ratcliffe RG, Sweetlove LJ, Fernie AR. 2005. Enhanced photosynthetic performance and growth as a consequence of decreasing mitochondrial malate dehydrogenase activity in transgenic tomato plants. *Plant Physiology* 137: 611–622.
- Nunes-Nesi A, Sweetlove LJ, Fernie AR. 2007. Operation and function of the tricarboxylic acid cycle in the illuminated leaf. *Physiologia Plantarum* 129: 45–56.
- Park AY, Canam T, Kang KY, Ellis DD, Mansfield SD. 2008. Over-expression of an *Arabidopsis* family A sucrose phosphate synthase (SPS) gene alters plant growth and fibre development. *Transgenic Research* 17: 181–192.
- Peeters N, Small I. 2001. Dual targeting to mitochondria and chloroplasts. *Biochimica Et Biophysica Acta-Molecular Cell Research* 1541: 54–63.
- Polge C, Jossier M, Crozet P, Gissot L, Thomas M. 2008. Beta-subunits of the SnRK1 complexes share a common ancestral function together with expression and function specificities; physical interaction with nitrate reductase specifically occurs via AKINbeta1-subunit. *Plant Physiology* 148: 1570–1582.
- Portis AR. 2003. Rubisco activase – Rubisco's catalytic chaperone. *Photosynthesis Research* 75: 11–27.

- Portis AR Jr, Li C, Wang D, Salvucci ME. 2008. Regulation of Rubisco activase and its interaction with Rubisco. *Journal of Experimental Botany* 59: 1597–1604.
- del Pozo JC, Allona I, Rubio V, Leyva A, de la Pena A, Aragoncillo C, Paz-Ares J. 1999. A type 5 acid phosphatase gene from *Arabidopsis thaliana* is induced by phosphate starvation and by some other types of phosphate mobilising/oxidative stress conditions. *Plant Journal* 19: 579–589.
- Rolland F, Baena-Gonzalez E, Sheen J. 2006. Sugar sensing and signaling in plants: conserved and novel mechanisms. *Annual Review of Plant Biology* 57: 675–709.
- Rolland F, Moore B, Sheen J. 2002. Sugar sensing and signaling in plants. *Plant Cell* 14: S185–S205.
- Saitou N, Nei M. 1987. The neighbor-joining method: a new method for reconstructing phylogenetic trees. *Molecular Biology and Evolution* 4: 406–425.
- Schenk G, Guddat LT, Ge Y, Carrington LE, Hume DA, Hamilton S, de Jersey J. 2000. Identification of mammalian-like purple acid phosphatases in a wide range of plants. *Gene* 250: 117–125.
- Schliebner I, Pribil M, Zuhlke J, Dietzmann A, Leister D. 2008. A survey of chloroplast protein kinases and phosphatases in *Arabidopsis thaliana*. *Current Genomics* 9: 184–190.
- Shapiguzov A, Ingelsson B, Samol I, Andres C, Kessler F, Rochoaix JD, Vener AV, Goldschmidt-Clermont M. 2010. The PPH1 phosphatase is specifically involved in LHCI dephosphorylation and state transitions in *Arabidopsis*. *Proceedings of the National Academy of Sciences, USA* 107: 4782–4787.
- Sharma-Natu P, Ghildiyal M. 2005. Potential targets for improving photosynthesis and crop yield. *Current Science* 88: 1928.
- Shen W, Hanley-Bowdoin L. 2006. Geminivirus infection up-regulates the expression of two *Arabidopsis* protein kinases related to yeast SNF1- and mammalian AMPK-activating kinases. *Plant Physiology* 142: 1642–1655.
- Shen W, Reyes MI, Hanley-Bowdoin L. 2009. *Arabidopsis* protein kinases GRIK1 and GRIK2 specifically activate SnRK1 by phosphorylating its activation loop. *Plant Physiology* 150: 996–1005.
- Siedlecka A, Ciereszko I, Mellerowicz E, Martz F, Chen J, Kleczkowski L. 2003. The small subunit ADP-glucose pyrophosphorylase (ApS) promoter mediates okadaic acid-sensitive uidA expression in starch-synthesizing tissues and cells in *Arabidopsis*. *Planta* 217: 184–192.
- Sienkiewicz-Porzucek A, Nunes-Nesi A, Sulpice R, Lisec J, Centeno DC, Carillo P, Leisse A, Urbanczyk-Wochniak E, Fernie AR. 2008. Mild reductions in mitochondrial citrate synthase activity result in a compromised nitrate assimilation and reduced leaf pigmentation but have no effect on photosynthetic performance or growth. *Plant Physiology* 147: 115–127.
- Sienkiewicz-Porzucek A, Sulpice R, Osorio S, Krahnert I, Leisse A, Urbanczyk-Wochniak E, Hodges M, Fernie AR, Nunes-Nesi A. 2010. Mild reductions in mitochondrial NAD-dependent Isocitrate dehydrogenase activity result in altered nitrate assimilation and pigmentation but do not impact growth. *Molecular Plant* 3: 156–173.
- Smeekens S, Ma J, Hanson J, Rolland F. 2010. Sugar signals and molecular networks controlling plant growth. *Current Opinion in Plant Biology* 13: 274–279.
- Studart-Guimaraes C, Fait A, Nunes-Nesi A, Carrari F, Usadel B, Fernie AR. 2007. Reduced expression of succinyl-coenzyme A ligase can be compensated for by up-regulation of the gamma-aminobutyrate shunt in illuminated tomato leaves. *Plant Physiology* 145: 626–639.
- Sugden C, Crawford RM, Halford NG, Hardie DG. 1999. Regulation of spinach SNF1-related (SnRK1) kinases by protein kinases and phosphatases is associated with phosphorylation of the T loop and is regulated by 5'-AMP. *Plant Journal* 19: 433–439.
- Sulpice R, Sienkiewicz-Porzucek A, Osorio S, Krahnert I, Stitt M, Fernie AR, Nunes-Nesi A. 2010. Mild reductions in cytosolic NADP-dependent isocitrate dehydrogenase activity result in lower amino acid contents and pigmentation without impacting growth. *Amino Acids* 39: 1055–1066.
- Takeda S, Mano S, Ohto M, Nakamura K. 1994. Inhibitors of protein phosphatases 1 and 2A block the sugar-inducible gene expression in plants. *Plant Physiology* 106: 567.
- Toroser D, Athwal GS, Huber SC. 1998. Site-specific regulatory interaction between spinach leaf sucrose-phosphate synthase and 14-3-3 proteins. *FEBS Letters* 435: 110–114.
- Tse YC, Mo B, Hillmer S, Zhao M, Lo SW, Robinson DG, Jiang L. 2004. Identification of multivesicular bodies as prevacuolar compartments in *Nicotiana tabacum* BY-2 cells. *Plant Cell* 16: 672–693.
- Ward JL, Harris C, Lewis J, Beale MH. 2003. Assessment of 1H NMR spectroscopy and multivariate analysis as a technique for metabolite fingerprinting of *Arabidopsis thaliana*. *Phytochemistry* 62: 949–957.
- Winter H, Huber J, Huber S. 1997. Membrane association of sucrose synthase: changes during the graviresponse and possible control by protein phosphorylation. *FEBS Letters* 420: 151–155.
- Worden AZ, Lee JH, Mock T, Rouze P, Simmons MP, Aerts AL, Allen AE, Cuvelier ML, Derelle E, Everett MV *et al.* 2009. Green evolution and dynamic adaptations revealed by genomes of the marine picoeukaryotes *Micromonas*. *Science* 324: 268–272.
- Wu F, Yang F, Vinnakota KC, Beard DA. 2007. Computer modeling of mitochondrial tricarboxylic acid cycle, oxidative phosphorylation, metabolite transport, and electrophysiology. *Journal of Biological Chemistry* 282: 24525–24537.
- Xu J, Avigne WT, McCarty DR, Koch KE. 1996. A similar dichotomy of sugar modulation and developmental expression affects both paths of sucrose metabolism: evidence from a maize invertase gene family. *Plant Cell* 8: 1209–1220.
- Yu XD, Sukumaran S, Marton L. 1998. Differential expression of the *Arabidopsis* Nia1 and Nia2 genes – cytokinin-induced nitrate reductase activity is correlated with increased Nia1 transcription and mRNA levels. *Plant Physiology* 116: 1091–1096.
- Zheng Z, Xu X, Crosley RA, Greenwalt SA, Sun Y, Blakeslee B, Wang L, Ni W, Sopko MS, Yao C *et al.* 2010. The protein kinase SnRK2.6 mediates the regulation of sucrose metabolism and plant growth in *Arabidopsis*. *Plant Physiology* 153: 99–113.
- Zhu HF, Qian WQ, Lu XZ, Li DP, Liu X, Liu KF, Wang DW. 2005. Expression patterns of purple acid phosphatase genes in *Arabidopsis* organs and functional analysis of AtPAP23 predominantly transcribed in flower. *Plant Molecular Biology* 59: 581–594.
- Zhu JM, Chen SX, Alvarez S, Asirvatham VS, Schachtman DP, Wu YJ, Sharp RE. 2006. Cell wall proteome in the maize primary root elongation zone. I. Extraction and identification of water-soluble and lightly ionically bound proteins. *Plant Physiology* 140: 311–325.

Supporting Information

Additional supporting information may be found in the online version of this article.

Fig. S1 Phylogenetic analysis of full length AtPAP2 protein sequence with related proteins in the other plant species.

Fig. S2 Amino acid sequence alignment of AtPAP2 with its homologous sequences from other plants.

Fig. S3 Verification of *AtPAP2* T-DNA mutant line.

Fig. S4 Western blot analysis of AtPAP2 in *Arabidopsis* tissues.

Fig. S5 Expression of AtPAP2 under various treatments.

Fig. S6 Growth phenotypes of genetically modified *Arabidopsis*.

Fig. S7 The TMD/CT region of AtPAP2 contains targeting signal to mitochondria.

Fig. S8 AtPAP2-GFP constructs did not co-localize with ER or Golgi markers.

Fig. S9 AtPAP2-GFP constructs did not co-localize with peroxisome marker.

Fig. S10 Analysis of SnRK1 proteins.

Fig. S11 Principal component analysis of $^1\text{H-NMR}$ data and GC-MS data.

Table S1 Signature motifs of AtPAP2-like proteins

Table S2 Relative metabolite content of shoots of 20-d-old AtPAP2 OE lines

Table S3 Primers used in this study

Please note: Wiley-Blackwell are not responsible for the content or functionality of any supporting information supplied by the authors. Any queries (other than missing material) should be directed to the *New Phytologist* Central Office.



About *New Phytologist*

- *New Phytologist* is an electronic (online-only) journal owned by the New Phytologist Trust, a **not-for-profit organization** dedicated to the promotion of plant science, facilitating projects from symposia to free access for our Tansley reviews.
- Regular papers, Letters, Research reviews, Rapid reports and both Modelling/Theory and Methods papers are encouraged. We are committed to rapid processing, from online submission through to publication 'as ready' via *Early View* – our average time to decision is <25 days. There are **no page or colour charges** and a PDF version will be provided for each article.
- The journal is available online at Wiley Online Library. Visit **www.newphytologist.com** to search the articles and register for table of contents email alerts.
- If you have any questions, do get in touch with Central Office (np-centraloffice@lancaster.ac.uk) or, if it is more convenient, our USA Office (np-usaoffice@ornl.gov)
- For submission instructions, subscription and all the latest information visit **www.newphytologist.com**